

A Silicon Photonic Switching Platform for Flexible Converged Centralized-Radio Access Networking

Colm Browning, Qixiang Cheng, Nathan C. Abrams, Marco Ruffini,
Liang Yuan Dai, Liam P. Barry and Keren Bergman

Abstract—Unprecedented levels of device connectivity and the emergence of futuristic digital services are driving fundamental changes to underlying fixed and wireless data transport networks. Projected bandwidth requirements, coupled with increased network centralization and virtualization, will lead to the convergence of data-center, fixed and wireless systems, and a greater onus being placed on the optical routing/transport portion of these networks. Such converged networks will require the development of optical technologies capable of servicing a multitude of network user types. In this work, we propose the use of a Silicon Photonic (SiP) space-and-wavelength selective switch fabric as a flexible wavelength provisioning platform for converged optical networks. The envisaged converged network is presented, and an experimental test-bed which demonstrates flexible Cloud Radio Access Networking (C-RAN), using a 4×4 micro-ring resonator based switch, is described. Successful provisioning and transmission of Wavelength Division Multiplexed (WDM) based analog Radio-over-Fiber (RoF) services, over 10 km of fiber, in the converged test-bed is demonstrated and evaluated in terms of the received Bit Error Rate (BER) and Error Vector Magnitude (EVM). Furthermore, the wavelength multi-casting capabilities of the SiP switch is shown to enable dynamic resource allocation in the optical domain, and this is highlighted through the experimental implementation and evaluation of two C-RAN use cases - representing high and low mobile traffic demand scenarios.

I. INTRODUCTION

ENHANCED mobile connectivity, and the proliferation of smart devices, continues to drive global internet traffic growth. It is forecast that by 2022, 71% of all IP traffic will be delivered wirelessly, either thorough mobile or Wi-Fi connections [1]. It is noteworthy that the report from Cisco [1] concludes by stating that next generation networks require “greater service portability and interoperability”, while also highlighting that future networks need to allow mobile devices

This publication has emanated from research supported by a research grant from Science Foundation Ireland (SFI) under grant number 18/SIRG/5579, and is co-funded under the European Regional Development Fund under grant number 15/US-C2C/I3132. This work was also supported in part by the U.S. Department of Energy Advanced Research Projects Agency—Energy under ENLIGHTENED Grant DE-AR000843.

C. Browning and L.P. Barry are with the School of Electronic Engineering, Dublin City University, Dublin D09W6Y4, Ireland. e-mail: colm.browning@dcu.ie

N. C. Abrams, Liang Yuan Dai and K.Bergman are with the with Department of Electrical Engineering, Columbia University, New York, NY 10027, USA.

Qixiang Cheng is with Electrical Engineering Division, Engineering Department, University of Cambridge, 9, JJ Thomson Avenue, Cambridge CB3 0FA, UK

M. Ruffini is with the CONNECT Research Centre at Trinity College Dublin, Dunlop Oriel House, Westland Row, Dublin 2.

Manuscript received...

“to be connected transparently with the network providing high-performance computing and delivering enhanced real-time video and multimedia”. It is clear that in order to deliver such advanced mobile services to a greater number of connected users, transport networks must not only evolve to offer higher bandwidth and lower latency, but will be required to provide flexible service delivery - ultimately leading to increased interoperability of mobile, Wi-Fi, fixed and cloud networks.

Centralized Radio Access Networks (C-RAN) is a highly promising technology for meeting long-term mobile network demands by enabling efficient transport and increased Network Function Virtualization (NFV) [2]. C-RAN involves the consolidation of radio-access/mobile network equipment at a Central Office (CO), typically linked to remote antenna sites by optical fiber. These links can be categorized as fronthaul, backhaul or midhaul (X-haul) depending on the type of functional split implemented (i.e., the amount of processing functionalities carried out at the remote antenna unit versus those at the CO). Current fiber-based fronthaul solutions consist of basic short-reach point-to-point links between a Baseband Unit (BBU) located at the antenna site, and a Remote Radio Head (RRH) typically located on a mast. But this implementation is viewed as un-sustainable as moving into the 5G era and beyond, will involve a vast deployment of small cell RRHs [3] - introducing major scalability issues, from an economic perspective. Migration to C-RAN architecture involving optical networking functionality brings with it the advantage of significant cost savings [4] as it facilitates high bandwidth connections, over 10’s of kilometers, to/from centralized BBU equipment.

As the mobile landscape moves towards ultra-dense deployment, the optical X-haul becomes key for supporting scalability and flexibility in delivering a multitude of new high-bandwidth services, including Virtual/Augmented Reality (VR/AR) and Autonomous Vehicle (AV) control. To meet these challenges, advances in flexible optical networking can be harnessed by C-RAN, and this will require closer alignment to, and integration with, surrounding intelligent optical networks - a concept known as network *convergence* [5], [6].

From the computing perspective, the augmentation of data center (DC) networks continues to facilitate the development and provisioning of powerful cloud-based mobile services to end-users. Indeed, it follows that DCs have been proposed as a suitable location for the placement of centralized C-RAN computing equipment [7], [8]. Such network convergence also offers the potential for flexible co-operation between C-RAN

and DC systems, by enabling network virtualization, whereby the BBU functionality can be dynamically implemented on powerful servers within the DC.

All-optical switching within the DC is an enabler for dynamic and high bandwidth data transfer in the fronthaul link, between virtualized (V-)BBUs and RRHs. But this can raise issues around the compatibility and co-management of various types of services and networking elements which are connected through a single switch fabric. Specifically, the ability to modulate and route a variety of network specific waveforms with shared transceiver equipment, and dynamic wavelength provisioning among converged network sectors, presents significant challenges both on a higher layer network control, and sub-system, level.

Optical fronthaul currently makes use of the Non Return-to-Zero (NRZ) modulation format. This looks set to be sustained in the near future as the recently standardised Enhanced Common Public Radio Interface (eCPRI) [9] allows currently deployed systems to harness Ethernet technology to meet near-term demands. However, as RAN capacity limitations are reached, it is inevitable that more advanced modulation will be utilized. This is an active area of research with the benefits and trade-offs associated with Analog RoF (A-RoF) and Digital RoF (D-RoF) being widely discussed [10]–[12].

Recent works have demonstrated the advantages that newly developed optical components and technologies can bring to RoF systems and converged optical networks. In particular, Silicon Photonics (SiP) has been identified as a key enabling platform which, through ease of integration and compatibility with CMOS processes, will greatly help to future-proof 5G transport networks [8], [13], [14]. Adding to this SiP's highly discussed potential to augment optical networking capabilities and throughput in DC interconnects [15], it is easy to see the attraction of the platform in the context of a converged optical network. Our previous work [16] has demonstrated the ability of a differential drive SiP Mach-Zehnder Modulator (MZM) to support efficient A-RoF service provisioning, while [17] describes and experimentally evaluates a fully integrated A-RoF transceiver on a SiP platform. [18] describes flexible wavelength routing using a polarization insensitive SiP Reconfigurable Optical Add Drop Multiplexer (ROADM) based on tunable Micro-ring Resonators (MRR). The device is shown to support 10 Gb/s CPRI transmission on up to 12 Wavelength Division Multiplexed (WDM) channels. In [19], Ericsson propose a similar MRR based SiP 'mini-ROADM' which is specifically designed for use as a flexible WDM hub in a D-RoF based C-RAN architecture.

In this work we experimentally demonstrate the ability of a 4×4 SiP space-and-wavelength selective switch fabric to dynamically provision WDM based A-RoF services in a 'converged' optical system. Up to 10 bands of the multi-carrier format Generalized Frequency Division Multiplexing (GFDM), at intermediate frequencies between 1.6 and 3 GHz, are successfully provisioned through the fabric and transmitted over two separate 10 km fronthaul links. The MRR based switch, which was designed for flexible DC interconnects, is also shown to facilitate wavelength multi-casting/sharing among fronthaul links - indicating the switch's potential to

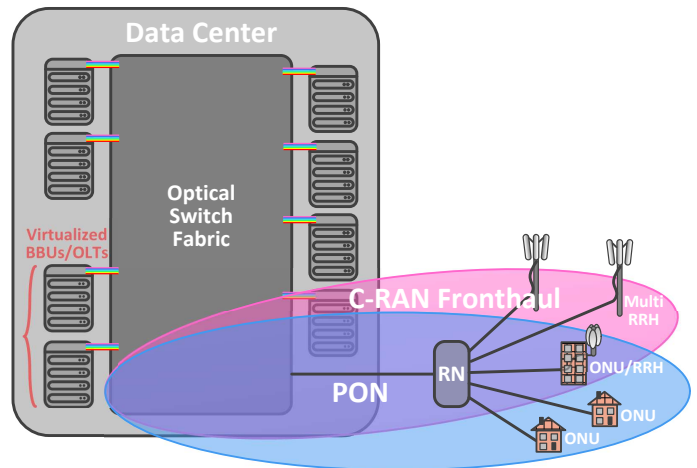


Fig. 1. Envisaged converged optical network.

support dynamic converged network optimization, in the optical domain.

II. ENVISAGED CONVERGED OPTICAL NETWORK

Increased network flexibility in the optical domain and the proposed co-location of radio and fixed access equipment will inevitably lead to greater convergence among cloud, access and mobile networks. Fig. 1 depicts our envisaged converged optical network architecture comprising a DC network, Passive Optical Network (PON) and a C-RAN. Network flexibility is provided mainly through the use of an optical switching fabric within the edge-DC which is located at the network periphery. Compared to a distributed cloud architecture, an edge-DC approach is preferred here for its potential to provide a low latency, time sensitive communications [20]. In the context of the envisaged converged network the DC provides the following functions:

- Acts as centralized location for the consolidation of RAN and PON equipment.
- Facilitates increased potential for network function virtualization, through DC server allocation.
- Provides a flexible optical networking platform to periphery networks by harnessing optical switching technologies developed for DC networking - the main focus of this work.

In the DC network, servers are connected to the switching fabric through the Top-of-Rack (TOR) which facilitates WDM operation by means of either tunable lasers or a laser array. The DC also houses centralized BBUs and Optical Line Terminals (OLT), which are used to provision services to deployed antenna sites and remote PON users (known as Optical Networking Units - ONUs), respectively. These network functional blocks, which may be realised as physical equipment, or virtualized within a server rack, interact flexibly with their respective transport networks by dynamic WDM connections to/from the optical switch fabric.

Fig. 1 shows converged C-RAN transport (pink) and Access (PON) transport (blue), linked to their respective central terminals in the DC. The concept of providing RoF

services over optical access (including PON) infrastructure is well explored, with the relevant technology types, for both analog and digital RoF over access implementations, defined in the ITU G-Series Recommendations [21], [22], which state that RoF service overlay “must be done by either operating in usable spectrum not occupied by legacy PONs in a particular deployment or re-using the legacy PON interfaces”. Other recent works have also proposed that future C-RAN deployment may be eased by leveraging next generation WDM-PON equipment/infrastructure [5], [23], [24]. The figure shows a converged PON/C-RAN infrastructure where connections, via demultiplexing at the Remote Node (RN), can be made to remotely deployed ONUs, multi-RRH sites or combined small cell RRHs/ONUs. It should be noted that, for the envisaged architecture proposed here, maximum flexibility through WDM networking can only be achieved if remote sites connected to a single C-RAN/PON can be dynamically assigned wavelength channels provisioned from the DC switch fabric. Practically, this can be realised in one of two ways;

RN Option I: The C-RAN/PON RN can be replaced by a Reconfigurable Arrayed Waveguide Grating (R-AWG) or mini-ROADM - allowing dynamic connectivity at the RN stage.

RN Option II: The RN is implemented as a simple passive power splitting element, and each remotely deployed optical receiver is fitted with a tunable optical filter [25]. This option simplifies C-RAN service delivery/overlay with currently deployed PON, but is detrimental to the achievable power budget compared to Option 1 - limiting the potential for network scaling.

Clearly, the optical switch fabric is the key technology offering WDM flexibility in (and between) converged network sectors, by providing a controllable dynamic space-and-wavelength switching platform. The work described here harnesses this DC based platform for wireless service provisioning over a converged PON infrastructure - as these network types remain the main high speed broadband resource, and whose proliferation continues today [26]. However, the advantages offered by such wavelength flexibility can be applied to any optical access technology for broadband or converged RoF transport. Optical switching for inter and intra-DC transmission has been the subject of much research and development over the past few years, with SiP emerging as the leading technology for large-scale optical switching platforms [27], [28]. The following section will detail the MRR based SiP switch used for the experimental work.

III. OPTICAL SWITCH FABRIC

The switch-and-select architecture, which is the basis for the design of the chip used in this work, comprises two linear switching arrays connected by a passive central shuffle network. Each $1 \times N/N \times 1$ switching unit is assembled by using MRR add-drop filters in a $1 \times N$ bus structure acting as spatial

(de)multiplexers. In this topology, the switching unit has a pair of MRRs (one in each linear array) dedicated to a specific input/output path - offering strictly non-blocking connectivity.

The silicon 4×4 MRR-based switch-and-select layout is shown schematically in Fig. 2(a). This device is similar to the one reported in [29], but with all elements fabricated in the silicon layer. It has 32 thermo-optic MRRs whose resonances can be tuned using associated integrated microheaters. Optical terminations are placed at each through port in order to eliminate reflections. A perfect shuffle is used to connect the 16 (4×4 arrays) MRRs at the input stage to the 16 MRRs at the output stage. Multi-mode based waveguide crossings are placed at the intersections for low-loss and low-crosstalk. A grating coupler array is used to couple light to and from the chip which was designed for TE-mode operation only.

The device was taped out using standard Process Design Kit (PDK) elements through the AIM Photonics Multi-Project Wafer (MPW) run. A microscopic photograph of the fabricated device is shown in Fig. 2(b). The thermo-optic MRRs are placed at a pitch of $100 \mu\text{m}$ to minimize thermal crosstalk. Their measured resonance shift shows a thermal efficiency of 1 nm/mW [30], and the 3 dB passbands of the MRRs are measured to be $\sim 24 \text{ GHz}$ [29]. The switch fabric has a compact footprint of $1.6 \times 2.5 \text{ mm}^2$ with 34 electrical bonding pads. The device was die-bonded onto a chip carrier and clamped on a custom PCB fan-out board. Finally, a fiber-array was UV-curved on the top surface of the silicon chip, and coupling was achieved via the grating coupler array which has a standard pitch of $127 \mu\text{m}$.

IV. USE CASES AND EXPERIMENTAL SETUP

A. Use Cases

The experimental work presented in this paper is designed to evaluate the following two downlink C-RAN wavelength provisioning use cases. Both use cases, which are enabled by

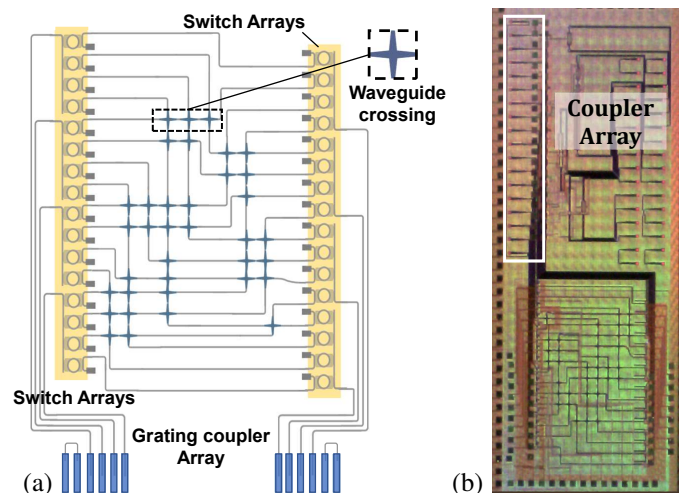


Fig. 2. (a) 4×4 MRR-based switch-and-select layout and (b) microscopic photograph of the fabricated device.

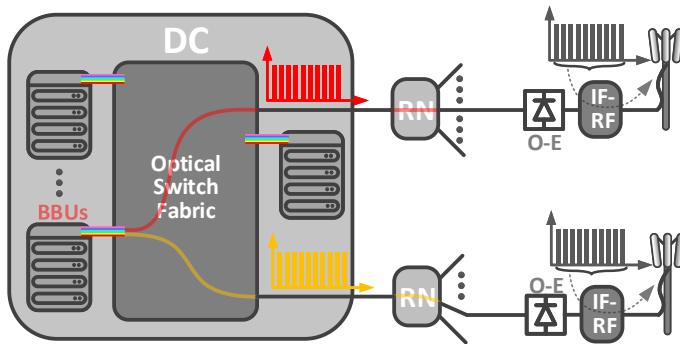


Fig. 3. Use Case 1 - dedicated wavelength per multi-RRH site, provisioned over a converged optical network.

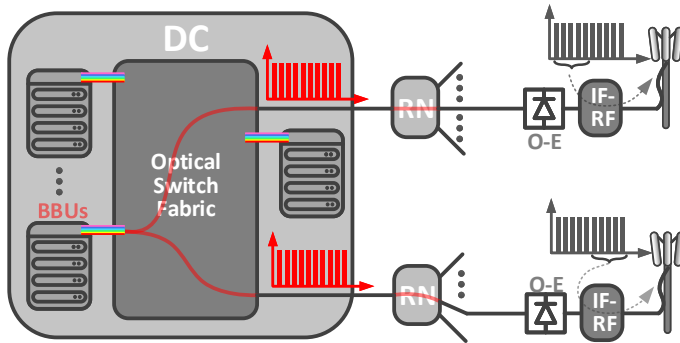


Fig. 4. Use Case 2 - A single wavelength, multi-cast to two multi-RRH sites over a converged optical network.

the switch fabric, are outlined in Figs. 3 and 4.

Case 1 - Full Service: In times of high demand, provisioning a dedicated wavelength channel per multi-RRH site can help to maximize C-RAN downlink capacities. Fig. 3 shows two converged C-RAN fronthaul links which each receiving a dedicated wavelength, provisioned from the V-BBU’s TOR through the MRR switch fabric which is configured accordingly. Each wavelength is modulated with independent IF A-RoF fiber services. At the multi-RRH site, the signal is converted to the electrical domain by a photo-receiver. At this stage all transmitted A-RoF channels are converted from IFs to the required RFs (using tunable microwave LOs) and directed to the appropriate RRH.

Case 2 - Partial Service: As demand decreases, the MRR switch can be configured to allow A-RoF services on a single wavelength to be split among the fronthaul links, as depicted in Fig. 4. This switch operation - which is known as optical multi-casting - is described in more detail in Section IV-C below. In this use case, the same set of IF A-RoF services are provisioned to both C-RAN multi-RRH sites, on the same wavelength. After optical-to-electrical (OE) conversion, a subset of IF channels (which have been assigned by the corresponding V-BBU) can be selected through tunable IF-RF conversion. The advantage here is that the drop in demand over the C-RAN is exploited in order to save a wavelength resource compared to ‘Case 1’. This

wavelength can then be re-provisioned by the switch fabric elsewhere in converged network. This comes at the cost of decreased optical power budget in fronthaul links, and this is discussed in Section V below.

B. Optical System

The experimental setup shown in Fig. 5, is designed to emulate the flexible C-RAN service provisioning envisaged in the architecture presented in Figs. 3 and 4. At the CO/DC side, light is emitted from a C-band Tunable Laser (TL) at a power of +10dBm, and passed to a single ended MZM via a Polarization Controller (PC). Multiple analog GFDM signals at IFs between 1.6 and 3 GHz (described in more detail in section IV-D) are output from an Arbitrary Waveform Generator (AWG) operating at 60 GSa/s. This electrical data signal is amplified and used to drive the MZM. The modulated light signal is coupled to input port 1 of the SiP MRR based 4×4 switch. This input light signal is then routed to a desired output port by ensuring that it is dropped from the associated input and output MRRs as described in section III. In this experimental work, light was routed from input port ‘1’ to one of two output ports, denoted ‘1’ and ‘4’ in Fig. 5. This was implemented by applying appropriate voltage control signals to the micro-heaters associated with the MRRs which are relevant to the two possible input/output paths. Light at the output of the switch fabric is amplified using an Erbium Doped Fiber Amplifier (EDFA) in order to overcome losses of between 10-15 dB which are mainly attributed to fiber coupling to/from the SiP chip. Each output port is connected to a 10 km optical fronthaul link (C-RAN FH 1 and C-RAN FH 2). At the receiver side a Variable Optical Attenuator (VOA) is used to control the power falling on a 20 GHz PIN photo-diode. The received electrical signal is amplified and captured using a Real Time Oscilloscope (RTS) sampling at 100 GSa/s. Down-sampling and demodulation, as well as Bit Error Rate (BER) and Error Vector Magnitude (EVM) calculation, are performed offline.

C. Multi-Cast Operation

As discussed, each input and output switch port has an associated bus of 4 MRRs; one for each possible input/output path. By tuning the MRRs appropriately, wavelength channels can be directed to the desired output port. It is also possible to pass the same wavelength to multiple output ports - known as optical multi-casting. Practically, this is achieved by tuning the center wavelength of the pass-bands associated with two or more MRRs (which are on the same input port bus) such that they are partially overlapping. In doing so, as the input wavelength enters the MRR bus, its power is partially dropped through one MRR, while the residual light continues to propagate and is dropped at subsequent appropriately tuned MRRs in the bus. The exploitation of this functionality can only be achieved through precise tuning of the thermo-optic MRRs which must be incorporated higher layer electronic control. We have previously demonstrated multi-casting functionality on up to 3 output ports of a SiP MRR based switch enabled by

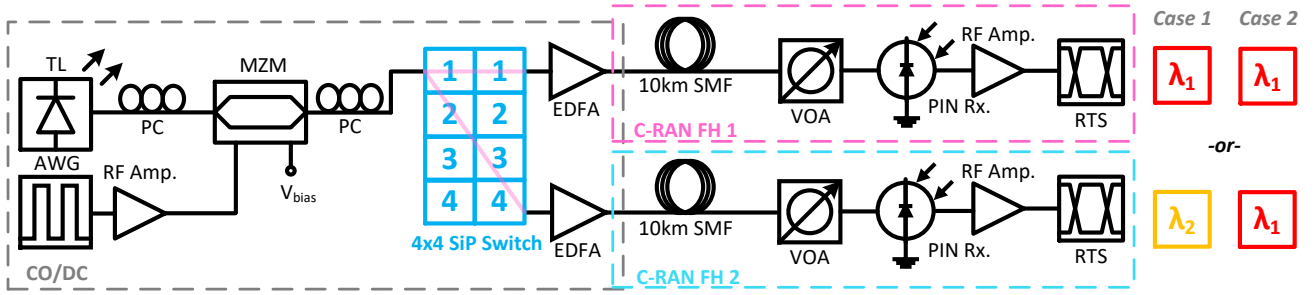


Fig. 5. Experimental setup indicating the two evaluated network scenarios.

the development of a scalable software defined control plane [31].

For the experimental work described here, optical multicasting provides the option of splitting a wavelength channel between two C-RAN fronthaul links. This scenario thereby allows for dynamic resource (wavelength) allocation at the DC, and this will be discussed in more detail in section V.

D. Analog Radio-over-Fiber Modulation

1) *A-RoF for Converged Fronthaul:* A-RoF represents a departure from currently deployed D-RoF technologies. Although it can suffer performance degradation in the presence of system non-linearities, when compared to digital RoF schemes, it provides vastly improved spectral efficiency and facilitates a reduction in remote hardware deployment - key properties which can facilitate the ultra dense small cell antenna deployment envisaged for future mobile systems. A-RoF’s amenability to network centralization, coupled with the proposed co-location of edge-DC and BBU pools, leads to a highly consolidated network implementation - helping to reduce OPEX through increased resource coordination. In the context of the envisaged network described here, effective techniques to pass A-RoF signals from the BBU (through the ToR) to the optical switch fabric are required. One potential solution would involve transmission from the BBU to the ToR in the form of I/Q samples over a Time Sensitive Networking (TSN) link (i.e. a low latency Ethernet link) to multiple Small Form-factor Pluggable (SFP) devices located at the ToR. In this scenario, the SFPs would be capable of transforming

the data streams into the appropriate A-RoF format and performing optical modulation. Wavelength multiplexing of multiple optical carriers can be performed at the ToR for WDM connection to the switch fabric.

2) *Signal Properties:* This experimental work makes use of the multi-carrier format GFDM. Compared to Orthogonal Frequency Division Multiplexing (OFDM) which will be employed at the outset of 5G, GFDM exhibits the same multi-carrier implementation but employs circular filtering which minimizes overlapping between subcarriers - increasing GFDM’s tolerance to timing synchronization errors, and making it a contending waveform for future 5G iterations [32].

Here, 10 bands of GFDM, per wavelength, are provisioned through the switch fabric to both fronthaul links. Each GFDM band contains 154 subcarriers which are modulated with 32 Quadrature Amplitude Modulation (QAM) at 977 kBaud and are multiplexed by an Inverse Fast Fourier Transform (IFFT). This results in a signal bandwidth of 150 MHz and a raw data rate of 0.75 Gb/s. Each of the 10 bands were digitally mixed to IFs ranging from 1.656 to 3.168 GHz which ensured a guard-band of ~10% of signal bandwidth between each GFDM band. The composite spectrum of 10 transmitted GFDM bands (total raw throughput of 7.5 Gb/s) is shown in 6(a).

V. RESULTS AND DISCUSSION

A. Use Case Implementation

The experimental setup shown in Fig. 5 was used to evaluate the two networking use cases discussed in Section IV-A.

Case 1 - Full Service: The MRRs at input port 1 are tuned so that λ_1 (194.3 THz) is directed to C-RAN FH 1, via output port 1, and λ_2 (194.8 THz) is directed to C-RAN FH 2, via output port 4. Both carriers are modulated with 10 IF A-RoF GFDM services. It should be noted that in this case, measurements for transmission through both output ports were performed in a piecemeal fashion i.e. λ_1 and λ_2 were not transmitted simultaneously in this proof-of-concept experiment.

Case 2 - Partial Service: Harnessing the optical multicasting functionality, MRRs in the bus associated with input port 1 are configured (in a manner outlined in IV-C) to provision the same modulated WDM channel (λ_1) to both

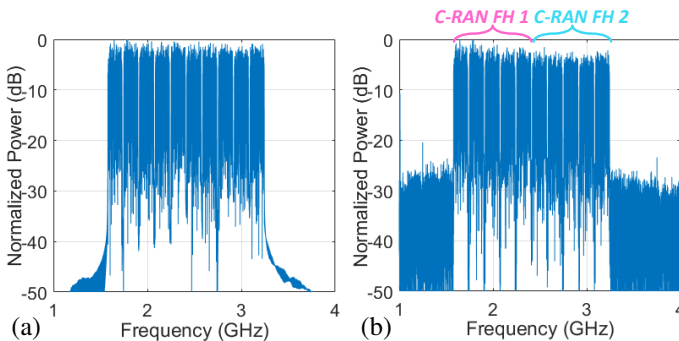


Fig. 6. Transmitted (a) and received (b) composite IF A-RoF GFDM spectra.

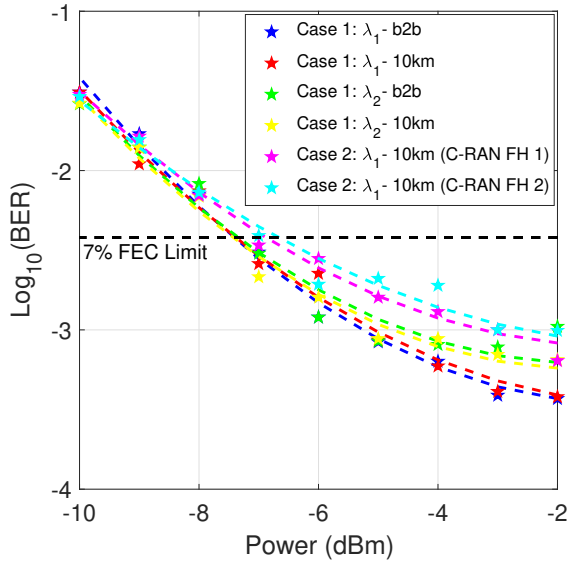


Fig. 7. Received optical power versus BER for ‘Case 1’ and ‘Case 2’ scenarios.

C-RAN FH 1 and C-RAN FH 2.

Fig. 6(b) shows an example spectra of 10 received IF GFDM services which have been multi-cast to both C-RAN links. In this example GFDM bands at IFs between 1.65 and 2.33 GHz are assigned to C-RAN FH 1, and those between 2.5 and 3.17 GHz to C-RAN FH 2. This operation, which requires co-operation between respective BBUs (virtualized, or otherwise) in the DC, allows λ_2 to be re-allocated to another portion of the converged optical network which requires increased capacity.

B. Performance

Fig. 7 shows received optical power versus the BER for ‘Case 1’, in back-to-back and 10 km scenarios, and ‘Case 2’ over 10 km SSMF. In all cases the BER was calculated based on a central GFDM band at an IF of 2.33 GHz. The optical power at the input to the fiber was maintained at +5 dBm.

For ‘Case 1’ results, the figure shows that there is no penalty between back-to-back and 10 km transmission for both WDM channels - indicating GFDM’s ability to deal effectively with fiber dispersion. At higher received powers there is a small performance penalty (~ 1 dB) between the two channels. This is due to the fact that as the λ_2 traverses the SiP switch from input port 1 to output port 4, it experiences 3-4 dB of extra loss compared to the pathway provisioned for λ_1 . This results in the requirement for additional EDFA gain in order to set the C-RAN FH 2 transmit power at + 5 dBm. A similar effect is evident for ‘Case 2’ transmission scenarios. The multi-casting operation effectively leads to a reduced Optical Signal-to-Noise Ratio (OSNR) as λ_1 ’s power is split between switch output ports. This manifests as a 2-3 dB penalty (compared to the ‘Case 1’ scenarios) at a received BER of 1×10^{-3} . The Forward Error Correction (FEC) BER threshold of 3.8×10^{-3}

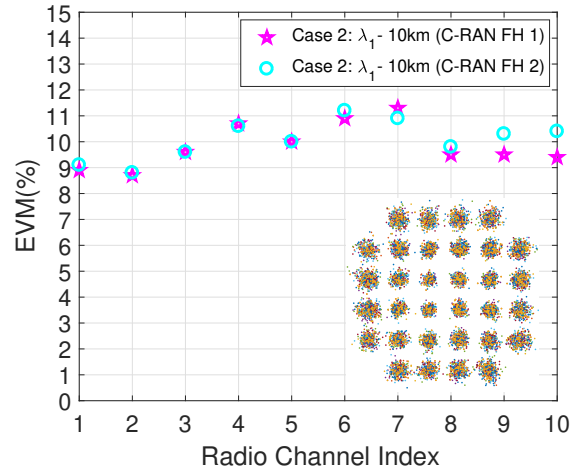


Fig. 8. Calculated EVM for each IF radio channel/band for both ‘Case 2’ scenarios.

is reached by all performance curves at ~ -7 dBm, as receiver noise begins to dominate system performance at this point.

For the setup configuration shown in Fig. 5, and for a target BER below the FEC threshold of 1×10^{-3} , a power budget of $\sim 14-15$ dB can be calculated for ‘Case 1’ scenarios. Considering that 3-4 dB should be reserved for 10 km transmission and connector losses, a sufficient budget is available to handle additional insertion and losses introduced by a WDM based RN. Compared to ‘Case 1’, the power budget for ‘Case 2’ transmission is reduced to ~ 12 dB. It should be noted that the system required a booster EDFA at the output of the SiP switch. Improvements in fiber coupling and/or the addition of an output Semiconductor Optical Amplifier (SOA) could negate the EDFA requirement for the proposed system.

The best performance is exhibited by λ_1 in ‘Case 1’ with a BER of 3.7×10^{-4} calculated at a received power of -2 dBm. At this power the worst performance, of 1×10^{-3} , is given by λ_1 when it is provisioned through output port 4 as prescribed in ‘Case 2’.

Fig. 8 shows the performance of each received IF GFDM radio channel/band, in terms of Error Vector Magnitude (EVM), where λ_1 is split between the two fronthaul links (‘Case 2’). In a practical implementation, the relevant subset of GFDM bands assigned to each link would be electronically extracted by the IF-RF conversion process, after photo-detection and before onward wireless transmission. However, for experimental demonstration purposes here, the performances of all 10 bands are evaluated having been multi-cast, transmitted and detected at the receive side of both C-RAN systems at -2 dBm. The figure shows that when the switch fabric is configured for optical multi-cast operation, very similar performances are observed across each received GFDM band, for both C-RAN fronthaul links. This uniformity in performance across both links is achieved by precise control of MRRs’ overlapping pass-bands [31], relative to the input wavelength, such that equal optical power is dropped at the output ports 1 and 4 - effectively equalizing optical power differentials which are due to variations in optical path losses between the chosen the

SiP switch routes.

Although all radio channels exhibit good performance, those located at central IFs experience a 1-2% degradation, in terms of EVM, compared to bands located at outer IFs. This is attributed to the fact that central bands will experience a higher level of interference from the Out-of-Band (OOB) emission spectra of surrounding GFDM bands. A contributory factor to the variations in performances between neighbouring bands is their relative transmitted electrical powers, which varied due to the bands' inherent Peak-to-Average Power Ratios (PAPR) - between 12 and 15 dB. The inset in Fig. 8 shows an example received 32-QAM constellation which was generated after the capture and down-conversion of radio channel 3 (IF = 2 GHz)

C. RoF Technologies for Converged Optical Networking

This work demonstrates the use of A-RoF transmission for fronthaul transmission which lends well to the key feature of resource *centralization* achieved by the proposed network design. However, D-RoF services (which are likely to be maintained in the coming years) could also be effectively provisioned. Compared to D-RoF, the analog approach is hindered by issues relating to its inherent large PAPR i.e. susceptibility to nonlinear distortion and inefficient use of electrical power amplifiers - leading to lower achievable wireless transmission distances. However, the improvement in spectral efficiency offered by A-RoF, compared to current D-RoF technology is enormous, particularly considering future network scaling. For example, currently deployed Common Public Radio Interface (CPRI) bit rate option 3 requires 2.457 Gb/s fronthaul transmission, while the user throughput is only 150 Mb/s [33]. With the inevitable scaling of this data rate, and the number of connected users, the required CPRI fronthaul transmission rates have the potential to reach to 100's Gb/s per cell, which is clearly unsustainable.

Of course, advances in D-RoF such as Enhanced (e)CPRI, and the use of higher order single carrier modulation formats, will go some way to alleviating this issue. But, as required wireless transmission distances are decreased through the proliferation of small cell antenna sites, and spectrally efficient optical fronthaul emerges as a critical part of the RAN, the benefits of A-RoF will begin to outweigh its drawbacks. Clearly there will be networking cases where either D-RoF or A-RoF are more beneficial, and interestingly, some research is proposing the coexistence of both fronthaul technologies by considering A-RoF as an additional functional split option in the RAN [34]. This is an interesting approach which could be used in tandem with the proposed network to provide enhanced flexibility.

With specific regard to the multi-casting functionality demonstrated in this work; D-RoF schemes would provide greater resilience in the presence of degraded SNR arising from power splitting among the switch MRRs. Nevertheless, A-RoF transmission provides the option of adapting the QAM modulation format used which can help to alleviate strict SNR requirements. Clearly this would result in reduced A-RoF fronthaul data rates, but could still provide a vast improvement in spectral efficiency over digital transmission schemes.

VI. CONCLUSION

The evolution toward networks capable of providing rich, data-hungry, services to our mobile devices will inevitably lead to the convergence of fixed, cloud and mobile networks. Specifically, the converged network architecture proposed here envisages close alignment of, and increased interaction between, DC, C-RAN and PON systems. Incorporating intelligent and flexible optical technologies into future deployments of these networks will be a key factor helping to sustain the growth in mobile capacities into the 5G era and beyond.

Network centralization and virtualization inside the DC provide a basis for the deployment of cost-effective, optically enabled C-RANs which will serve densely deployed antenna sites. The results presented in the paper show how a SiP MRR based switching fabric, designed for DC inter-connects, can also be used to flexibly provision A-RoF traffic out of the DC. Results also show how switch reconfiguration successfully provides multi-cast A-RoF services among C-RAN links, facilitating dynamic resource allocation in the optical domain. Overall, these results indicate how silicon photonics, with the aid of the development of scalable intelligent electronic control and network virtualization, can act as a linchpin large-scale integrated switching platform in future flexible converged networks.

REFERENCES

- [1] Cisco, "Cisco Visual Networking Index: Global Mobile Data Traffic Forecast Update, 2017-2022," *White Paper*, 2019.
- [2] X. Wang, C. Cavdar, L. Wang, M. Tornatore, H. S. Chung, H. H. Lee, S. M. Park, and B. Mukherjee, "Virtualized cloud radio access network for 5g transport," *IEEE Communications Magazine*, vol. 55, no. 9, pp. 202-209, Sep. 2017.
- [3] C. Ranaweera, E. Wong, A. Nirmalathas, C. Jayasundara, and C. Lim, "5g c-ran with optical fronthaul: An analysis from a deployment perspective," *Journal of Lightwave Technology*, vol. 36, no. 11, pp. 2059-2068, June 2018.
- [4] C. Liu, J. Wang, L. Cheng, M. Zhu, and G. Chang, "Key microwave-photonics technologies for next-generation cloud-based radio access networks," *Journal of Lightwave Technology*, vol. 32, no. 20, pp. 3452-3460, Oct 2014.
- [5] A. Tzanakaki, M. P. Anastopoulos, and D. Simeonidou, "Converged optical, wireless, and data center network infrastructures for 5g services," *J. Opt. Commun. Netw.*, vol. 11, no. 2, pp. A111-A122, Feb 2019. [Online]. Available: <http://jocn.osa.org/abstract.cfm?URI=jocn-11-2-A111>
- [6] C. Browning, "Wired and wireless convergence in future optical access networks - invited," in *2019 IEEE Photonics Conference (IPC)*, Sep. 2019, pp. 1-2.
- [7] T. Pfeiffer, "Next generation mobile fronthaul and midhaul architectures - invited," *J. Opt. Commun. Netw.*, vol. 7, no. 11, pp. B38-B45, Nov 2015. [Online]. Available: <http://jocn.osa.org/abstract.cfm?URI=jocn-7-11-B38>
- [8] A. D. La Oliva, X. C. Perez, A. Azcorra, A. D. Giglio, F. Cavaliere, D. Tiegelbekkers, J. Lessmann, T. Hausteine, A. Mourad, and P. Iovanna, "Xhaul: toward an integrated fronthaul/backhaul architecture in 5g networks," *IEEE Wireless Communications*, vol. 22, no. 5, pp. 32-40, October 2015.
- [9] CPRI, "ecpri specification v2.0 (2019-05-10)," *Common Public Radio Interface: eCPRI Interface Specification*, 2019.
- [10] S. Noor, P. Assimakopoulos, and N. J. Gomes, "A flexible subcarrier multiplexing system with analog transport and digital processing for 5g (and beyond) fronthaul," *Journal of Lightwave Technology*, vol. 37, no. 14, pp. 3689-3700, July 2019.
- [11] L. Breynne, G. Torfs, X. Yin, P. Demeester, and J. Bauwelinck, "Comparison between analog radio-over-fiber and sigma delta modulated radio-over-fiber," *IEEE Photonics Technology Letters*, vol. 29, no. 21, pp. 1808-1811, Nov 2017.

- [12] C. Browning, A. Farhang, A. Saljoghei, N. Marchetti, V. Vujicic, L. E. Doyle, and L. P. Barry, "5g wireless and wired convergence in a passive optical network using uf-ofdm and gfdm," in *2017 IEEE International Conference on Communications Workshops (ICC Workshops)*, May 2017, pp. 386–392.
- [13] R. Sabella, "Silicon photonics for 5g and future networks," *IEEE Journal of Selected Topics in Quantum Electronics*, vol. 26, no. 2, pp. 1–11, March 2020.
- [14] B. Skubic, G. Bottari, A. Rostami, F. Cavaliere, and P. Öhlén, "Rethinking optical transport to pave the way for 5g and the networked society," *J. Lightwave Technol.*, vol. 33, no. 5, pp. 1084–1091, Mar 2015. [Online]. Available: <http://jlt.osa.org/abstract.cfm?URI=jlt-33-5-1084>
- [15] D. Nikolova, S. Rumley, D. Calhoun, Q. Li, R. Hendry, P. Samadi, and K. Bergman, "Scaling silicon photonic switch fabrics for data center interconnection networks," *Opt. Express*, vol. 23, no. 2, pp. 1159–1175, Jan 2015. [Online]. Available: <http://www.opticsexpress.org/abstract.cfm?URI=oe-23-2-1159>
- [16] C. Browning, A. Gazman, N. Abrams, K. Bergman, and L. P. Barry, "256/64-qam multicarrier analog radio-over-fiber modulation using a linear differential drive silicon mach-zehnder modulator," in *2018 International Topical Meeting on Microwave Photonics (MWP)*, Oct 2018, pp. 1–4.
- [17] K. Van Gasse, L. Bogaert, L. Breyne, J. Van Kerrebrouck, S. Dhoore, C. Op de Beeck, A. Katumba, C. Wu, H. Li, J. Verbist, A. Rahim, A. Abbasi, B. Moeneclaey, Z. Wang, H. Chen, J. Van Campenhout, X. Yin, B. Kuyken, G. Morthier, J. Bauwelinck, G. Torfs, and G. Roelkens, "Analog radio-over-fiber transceivers based on iii-v-on-silicon photonics," *IEEE Photonics Technology Letters*, vol. 30, no. 21, pp. 1818–1821, Nov 2018.
- [18] V. Sorianoello, G. D. Angelis, T. Cassese, M. V. Preite, P. Velha, A. Bianchi, M. Romagnoli, and F. Testa, "Polarization insensitive silicon photonic roadm with selectable communication direction for radio access networks," *Opt. Lett.*, vol. 41, no. 24, pp. 5688–5691, Dec 2016. [Online]. Available: <http://ol.osa.org/abstract.cfm?URI=ol-41-24-5688>
- [19] P. Iovanna, F. Cavaliere, F. Testa, S. Stracca, G. Bottari, F. Ponzini, A. Bianchi, and R. Sabella, "Future proof optical network infrastructure for 5g transport," *IEEE/OSA Journal of Optical Communications and Networking*, vol. 8, no. 12, pp. B80–B92, December 2016.
- [20] Ericsson, "Edge computing and deployment strategies for communication service providers," *White Paper*, 2020.
- [21] "Radio-over-fibre (rof) technologies and their applications," International Telecommunication Union, Standard, July 2015.
- [22] "5g wireless fronthaul requirements in a passive optical network," International Telecommunication Union, Standard, July 2015.
- [23] J. Kani, J. Terada, K. Suzuki, and A. Otaka, "Solutions for future mobile fronthaul and access-network convergence," *Journal of Lightwave Technology*, vol. 35, no. 3, pp. 527–534, Feb 2017.
- [24] D. Nasset, "Pon roadmap [invited]," *IEEE/OSA Journal of Optical Communications and Networking*, vol. 9, no. 1, pp. A71–A76, Jan 2017.
- [25] Z. Zhang, Y. Chen, S. Cai, B. Zhang, M. Zhang, and X. Chen, "Colorless-light and tunable-light-source schemes for twdm and wdm pons," *IEEE Communications Magazine*, vol. 56, no. 8, pp. 120–128, August 2018.
- [26] J. S. Wey, "The outlook for pon standardization: A tutorial," *Journal of Lightwave Technology*, vol. 38, no. 1, pp. 31–42, Jan 2020.
- [27] Q. Cheng, Y. Huang, H. Yang, M. Bahadori, N. Abrams, X. Meng, M. Glick, Y. Liu, M. Hochberg, and K. Bergman, "Silicon photonic switch topologies and routing strategies for disaggregated data centers," *IEEE Journal of Selected Topics in Quantum Electronics*, pp. 1–1, 2019.
- [28] M. C. Wu, T. J. Seok, K. Kwon, J. Henriksson, and J. Luo, "Large scale silicon photonics switches based on mems technology," in *2019 Optical Fiber Communications Conference and Exhibition (OFC)*, March 2019, pp. 1–3.
- [29] Q. Cheng, L. Y. Dai, N. C. Abrams, Y.-H. Hung, P. E. Morrissey, M. Glick, P. O'Brien, and K. Bergman, "Ultralow-crosstalk, strictly non-blocking microring-based optical switch," *Photon. Res.*, vol. 7, no. 2, pp. 155–161, Feb 2019. [Online]. Available: <http://www.osapublishing.org/prj/abstract.cfm?URI=prj-7-2-155>
- [30] M. Bahadori, A. Gazman, N. Janosik, S. Rumley, Z. Zhu, R. Polster, Q. Cheng, and K. Bergman, "Thermal rectification of integrated microheaters for microring resonators in silicon photonics platform," *Journal of Lightwave Technology*, vol. 36, no. 3, pp. 773–788, Feb 2018.
- [31] A. Gazman, C. Browning, M. Bahadori, Z. Zhu, P. Samadi, S. Rumley, V. Vujicic, L. P. Barry, and K. Bergman, "Software-defined control-plane for wavelength selective unicast and multicast of optical data in a silicon photonic platform," *Opt. Express*, vol. 25, no. 1, pp. 232–242, Jan 2017.
- [Online]. Available: <http://www.opticsexpress.org/abstract.cfm?URI=oe-25-1-232>
- [32] B. Farhang-Boroujeny and H. Moradi, "Ofdm inspired waveforms for 5g," *IEEE Communications Surveys Tutorials*, vol. 18, no. 4, pp. 2474–2492, Fourthquarter 2016.
- [33] G. Giannoulis, N. Argyris, N. Iliadis, G. Pouloupoulos, K. Kanta, D. Apostolopoulos, and H. Avramopoulos, "Analog radio-over-fiber solutions for 5g communications in the beyond-cpri era," in *2018 20th International Conference on Transparent Optical Networks (ICTON)*, July 2018, pp. 1–5.
- [34] N. J. Gomes and P. Assimakopoulos, "Optical fronthaul options for meeting 5g requirements," in *International Conference on Transparent Optical Networks*. IEEE, August 2018. [Online]. Available: <https://kar.kent.ac.uk/69102/>